Acceleration of Biexciton Radiative Recombination at Low Temperature in CdSe Nanoplatelets

Journal:	*Nano Letters*
Manuscript ID	nl-2022-01791w.R2
Manuscript Type:	Communication
Date Submitted by the Author:	n/a
Complete List of Authors:	Brumberg, Alexandra; Northwestern University, Chemistry Watkins, Nicolas; Northwestern University, Chemistry Diroll, Benjamin; Argonne National Laboratory, Nanoscience and Technology Schaller, Richard; Northwestern University, Department of Chemistry

Acceleration of Biexciton Radiative Recombination at Low Temperature in CdSe Nanoplatelets

Alexandra Brumberg,[1,†] Nicolas E. Watkins,[1] Benjamin T. Diroll,[2] and Richard D. Schaller[1,2,*]

[1] Department of Chemistry, Northwestern University, Evanston, IL 60208, USA

[2] Center for Nanoscale Materials, Argonne National Laboratory, Lemont, IL 60439, USA

* Corresponding author: schaller@northwestern.edu, schaller@anl.gov

† Present affiliation: Department of Materials Science & Engineering, University of California, Berkeley, CA 94710

Abstract

Colloidal semiconductor nanocrystals offer bandgap tunability, high photoluminescence quantum yield, and colloidal processing of benefit to optoelectronics, however rapid nonradiative Auger recombination (AR) deleteriously affects device efficiencies at elevated excitation intensities. AR is understood to transition from temperature-dependent behavior in bulk semiconductors to temperature-independent behavior in zero-dimensional quantum dots (QDs) as a result of discretized band structure that facilitates satisfaction of linear momentum conservation. For nanoplatelets (NPLs), two-dimensional morphology renders prediction of photophysical behaviors challenging. Here, we investigate and compare the temperature dependence of excited-stated lifetime and fluence-dependent emission of CdSe NPLs and QDs. For NPLs, upon temperature reduction, biexciton lifetime surprisingly *decreases* (even becoming shorter lived than trion emission) and emission intensity increases nearly linearly with fluence rather than saturating, consistent with dominance of radiative recombination rather than AR. CdSe NPLs thus differ fundamentally from core-only QDs and foster increased utility of photogenerated excitons and multiexcitons at low temperatures.

Keywords: nanoplatelets, biexcitons, Auger recombination, quantum yield, temperature-dependent emission

Semiconductor nanocrystals offer prospective use in optoelectronic applications such as light-emitting diodes (LEDs) and lasers. As these devices are operated at progressively higher powers to produce increased light output, nonradiative processes originating from Auger recombination (AR) of biexcitons occur alongside biexciton radiative recombination and reduce device efficiencies.[1–3] Auger recombination, in which an electron and a hole recombine and nonradiatively transfer their potential energy to a third carrier, is a putative mechanism through which *e.g.* LED efficiency rolls off as injection current is raised[2,4,5] and population inversion is rapidly reduced, hindering lasing.[6–9] In colloidal quantum dots (QDs), AR is faster than in bulk materials owing both to strong quantum confinement, which increases the electron-hole wavefunction overlap and Coulombic coupling, as well as the presence of abrupt interfaces.[10–14] Furthermore, in QDs, linear momentum is readily conserved owing to discretized energy levels rather than dispersive bands, such that rates of AR are chiefly prescribed by angular momentum conservation requirements and density of states considerations.[14,15] In contrast, for bulk semiconductors, the three carriers involved in AR must realize the low likelihood of simultaneously satisfying conservation of energy and linear momentum on curved dispersion bands.[16] As a result, rates of AR in QDs are orders of magnitude

faster than in bulk semiconductors, leading to ten- to hundred picosecond lifetimes[12,17] that impede the use of semiconductor QDs in devices. Examples of efforts to slow down rates of AR[18] and increase multiexciton emission include growth of a QD shell,[19–22] interfacial engineering,[9,23,24] and doping.[25]

Colloidal, two-dimensional semiconductor nanoplatelets (NPLs) offer an advantage regarding the problem of fast AR rates while preserving other benefits of QDs such as band gap tunability and high photoluminescence efficiency. NPLs feature reduced rates of AR,[26–28] which has led to many research efforts targeting incorporation of NPLs into LEDs and nanoscale lasers.[26,29–32] However, the mix of quantum-confined and bulk-like dimensions in NPLs along the thickness and lateral axes, respectively, makes it difficult to predict some photophysical behaviors. Comparison to well-studied epitaxial quantum wells is also not straightforward. In particular, core-only NPLs experience abrupt and significant changes in electronic potential owing to proximal organic ligands and solvent whereas epitaxial quantum wells, which require near-lattice matched semiconductor substrates, present less severe changes in bandgap and dielectric contrast.[33] Furthermore, both experimental and theoretical efforts have yet to agree on the relationship between AR rate and NPL area and volume.[26–28,34,35] Despite insightful literature investigations of AR in NPLs,[36–43] more studies are needed to understand multi-exciton processes in these structures. Most studies attribute fast recombination lifetimes at elevated fluences to AR based on literature precedent for QDs; however, disambiguating between AR and radiative recombination requires fluence-dependent PL that, until now, has not been reported for core-only colloidal NPLs.

In intrinsic bulk semiconductors, temperature reduction slows AR, as satisfaction of momentum conservation becomes progressively more difficult to fulfill.[15,16] In zero-dimensional QDs, carriers undergoing AR can achieve conservation of linear momentum at any temperature for discretized energy levels (though total angular momentum still must be conserved) and so AR rates are predicted to be independent of temperature.[15,44] In practice, however, some experimental measurements have suggested a phonon-assisted AR mechanism that leads to temperature-dependent rates for CdSe QDs below 175 °C.[45,46] These conservation of momentum requirements and their implications regarding AR are summarized in Figure 1. Given quantum confinement in one, but not all three dimensions, it remains unclear how AR rates will be affected by temperature in two-dimensional NPLs. Prior work on the temperature dependence of AR in epitaxial quantum wells indicates weak, if any, temperature sensitivity.[47–52]

Beyond fundamental relevance, the temperature dependence of AR rates also relates to the low temperature emission behavior of CdSe NPLs, which despite many investigations remains a subject of discussion. Below ~100 K, absorption of a single photon leads to dual peak emission in ensembles. While the higher energy peak is understood to correspond to emission of the neutral exciton, the origin of the lower energy emission peak is debated[53–56] with a majority of reports conveying that it arises from negative

trion emission.[55–58] This excess charge can be introduced via effects such as Auger ionization, in which the excited carrier promoted during AR gains sufficient energy to escape the particle; surface trapping, in which a carrier becomes trapped in a mid-gap state created by a surface defect; or n- or p-type doping. The hypothesis that the lower energy peak corresponds to trion emission suggests that the increased (trion) emission at lower temperatures is a result of reduced – or even negligible – rates of AR at cryogenic temperatures, for example as argued by Antolinez *et al.*[56] The temperature dependence of trion emission thus implies either a temperature dependence for AR, whereby rates of AR might decrease with decreasing temperature, as is the case for bulk semiconductors, or a temperature-dependent trion concentration. The only work thus far to measure Auger lifetimes as a function of temperature in NPLs identified a temperature independent Auger lifetime of ~3 ns for CdSe/CdS core/shell NPLs between 4.5 K and room temperature, more consistent with 0D structures.[59]

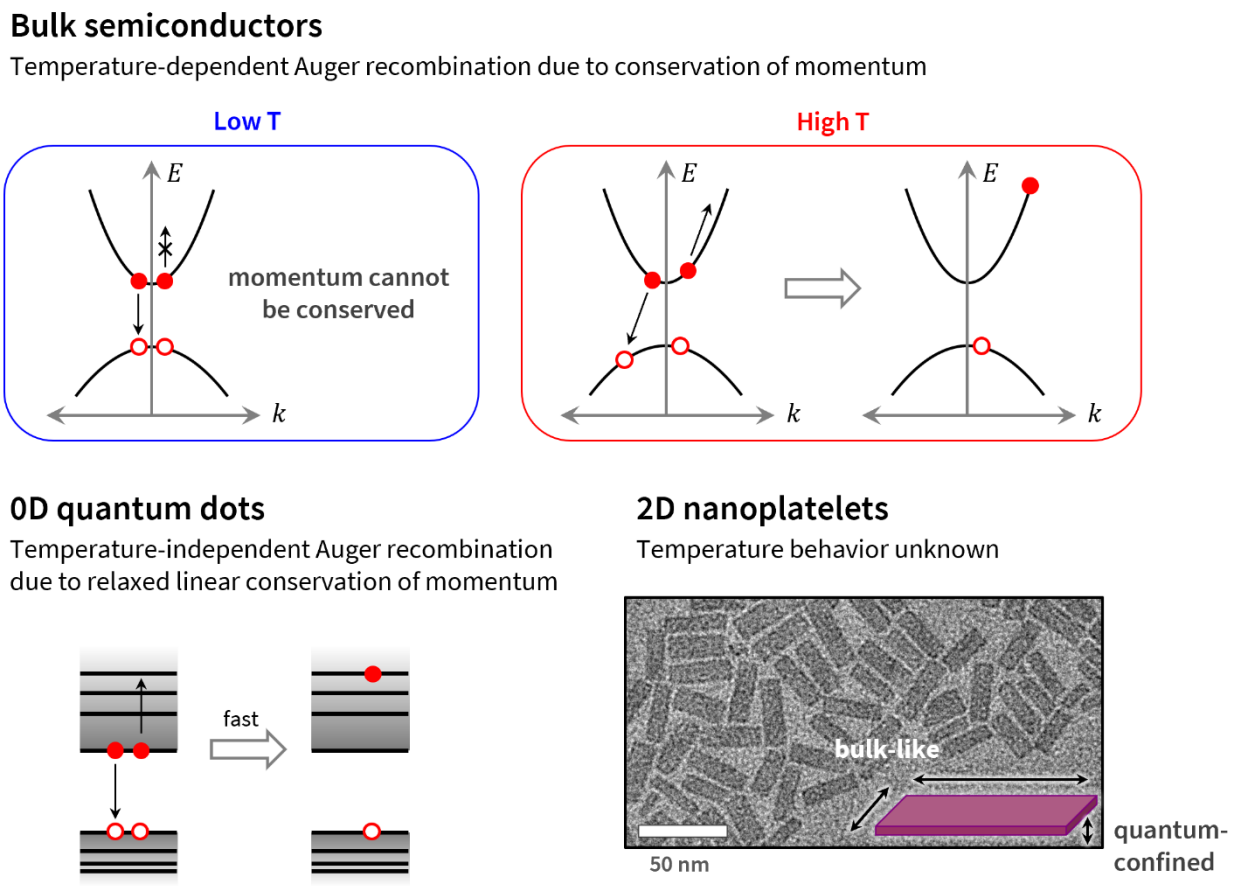

Figure 1. Depiction of Auger processes in bulk, direct bandgap intrinsic semiconductors *vs* nanocrystal forms and the impact of temperature on AR rates. In the bottom right, transmission electron microscopy (TEM) of representative 5.5 ML CdSe NPLs are shown.

In this work, we perform time-resolved photoluminescence (trPL) measurements as functions of temperature and pump fluence to characterize biexciton lifetime dependencies. Our results indicate that biexciton lifetimes are temperature-dependent in NPLs. Notably, however, the exhibited temperature dependence is distinct both from that observed in bulk semiconductors and in QDs; the biexciton lifetime decreases as temperature is lowered in CdSe NPLs. Through analysis of biexciton emission *vs.* pump fluence, we show that this decreased excited state lifetime arises at least in part due to increased biexciton radiative recombination rates at low temperatures. This work emphasizes that, despite the dominance of nonradiative multiexciton recombination at room temperature in QDs and NPLs, the behavior of non-zero-dimensional particles at low temperatures offers unique, technologically useful features.

CdSe NPLs with 5.5 monolayer (ML) thickness (five alternating layers of Cd^{2+} and Se^{2-}, terminated by Cd^{2+} on either side) were synthesized according to previously published procedures.[26,60] At room temperature, 5.5 ML CdSe NPLs exhibit a heavy hole exciton absorption peak at 550 nm and emission maximum at 554 nm (Figure S1). For comparison, zinc-blende CdSe QDs of a similar band gap were also prepared.[61] CdSe QDs and NPLs were dispersed in a 1:1 mixture of hexanes to methylcyclohexane by volume at an optical density of 0.2 to 0.3 at 400 nm in a 2 mm sapphire cuvette and loaded into a helium cryostat. Methylcyclohexane helps the dispersion to freeze as a glassy solid, and addition of hexanes was found to reduce cloudiness. Time-resolved PL measurements were performed using controlled-fluence 400 nm photons produced via the frequency-doubled output of a 35-fs Ti:sapphire laser operating at 2 kHz. Photoluminescence was collected, directed through a 420 nm long pass filter, dispersed using a 0.15 m spectrograph, and directed to a single-photon sensitive streak camera.

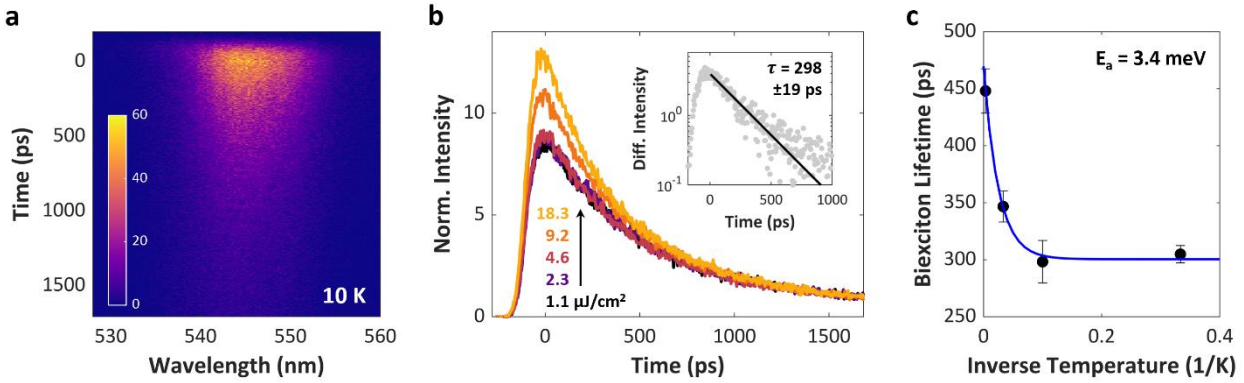

Figure 2. Fluence-dependent time-resolved PL of 5.5 ML thick CdSe NPLs dispersed in a 1:1 mixture of hexanes to methylcyclohexane. **(a)** Representative trPL data at 10 K. The color scale indicates number of detected photons per pixel. **(b)** Example trPL data at 10 K for a range of indicated fluences, integrated across the wavelength region of interest shown in (a) and normalized at late time (near 1500 ps). The biexciton lifetime was determined by subtracting such normalized single exciton dynamics from the higher power data. The result of the subtraction procedure, shown in the inset, yields monoexponential data that can be fitted to determine the biexciton lifetime. **(c)** Biexciton lifetime

as a function of inverse temperature shows that as the temperature drops, biexciton lifetime shortens. Solid line conveys a fit to the Arrhenius equation with an activation energy of 3.4 meV.

Figure 2 shows trPL measurements of 5.5 ML CdSe NPLs at 10 K acquired in a 2 ns time window for fluences between 1.1 and 18 μJ/cm^2. Raw data (Figure 2a) were integrated across all wavelengths to examine excited-state dynamics (Figure 2b). When normalized near 1.5 ns, trPL collected at 1.1 and 2.3 μJ/cm^2 exhibit the same dynamics, suggesting only single photoexcitations per particle. At higher fluences, differences in intensity appear between $t = 0$ and 500 ps compared to lower fluence data, consistent with multiexciton response. Thus, by normalizing the data around 1.5 ns, differences at earlier times emphasize signal from particles containing biexcitons *vs.* single excitons present as increased light intensity near $t = 0$. By differencing the normalized single exciton data collected at low powers, from the data collected at higher powers, where the average number of generated excitons per particle $\langle N \rangle$ is such that some of the excited NPLs contain biexcitons, the biexciton dynamics can be isolated. The differenced dynamics can then be fit to an exponential function to obtain a biexciton lifetime, the result of which is shown in the inset of Figure 2b. Data acquired at a power of 1.1 μJ/cm^2 were used for single exciton dynamics, while data acquired at 9.2 μJ/cm^2 here were used to discern biexciton dynamics.

The fitted biexciton dynamics measured for these CdSe NPLs at temperatures of 3, 10, 30, and 295 K appear in Figure 2c. With reduced temperature, the biexciton lifetime shortens, decreasing from 448 ±19 ps at room temperature to 305 ±8 ps at 3 K. This reduction of lifetime is distinct from both the temperature dependent scaling of AR lifetimes observed in bulk semiconductors, where AR lifetimes in the latter become longer as the temperature falls owing to lower probability of satisfying conservation of momentum, as well as inconsistency with temperature independent QDs. The atypical decrease of biexciton lifetime with decreasing temperature suggests an alternate mechanism. Rather than nonradiative AR serving as the dominant recombination mechanism for biexcitons in colloidal NPLs, radiative recombination may instead become dominant at lower temperatures and can explain the unexpected trend in lifetimes. Importantly, single excitons also exhibit temperature-dependent trends in NPLs, as has been previously reported.[55,60]

To test this radiative biexciton hypothesis, we conducted fluence-dependent, time-integrated PL measurements of CdSe NPLs at 10 K and 295 K, then compared the resultant PL intensities to determine the extent to which multiexcitons decay via radiative pathways. The results of these experiments are shown in Figure 3. In the single exciton regime where $\langle N \rangle \ll 0.1$, increasing the fluence simply changes the population of NPLs that are excited with one exciton. In this regime, the graph of the integrated PL intensity *vs*. fluence is linear. As we further increase fluence, excitation produces biexcitons in a population of NPLs, as prescribed by Poisson statistics. Naively, biexcitons radiate at approximately 4× the rate (i.e. with ¼ the lifetime) of single excitons, owing to the four possible electron-hole recombination pathways. As such, for

NPLs with an 8 ns single exciton radiative lifetime at room temperature,[62] the biexciton radiative lifetime would be expected to equal 2 ns. Since observed NPL biexciton lifetimes at this temperature are on the order of hundreds of picoseconds (tens of picoseconds for QDs, for which single exciton radiative lifetimes are even longer), biexciton decay must be predominantly nonradiative. Accordingly, Figures 3a and 3c for NPLs and QDs, respectively, show that the integrated PL intensity saturates with increasing pump fluence, consistent with multiexcitons predominantly undergoing nonradiative AR and single exciton emission dominating the measured radiative emission. Saturation occurs according to $1 - p_0$, where p_0 is the Poissonnian fraction of unexcited NPLs. At sufficiently high fluence, essentially all NPLs in the excitation spot contain at least 1 photoexcitation; however, only one of these photoexcitations leads to efficient photoluminescence following AR, resulting in the $1 - p_0$ saturation behavior marked in Figures 3a and 3c by the dashed lines.

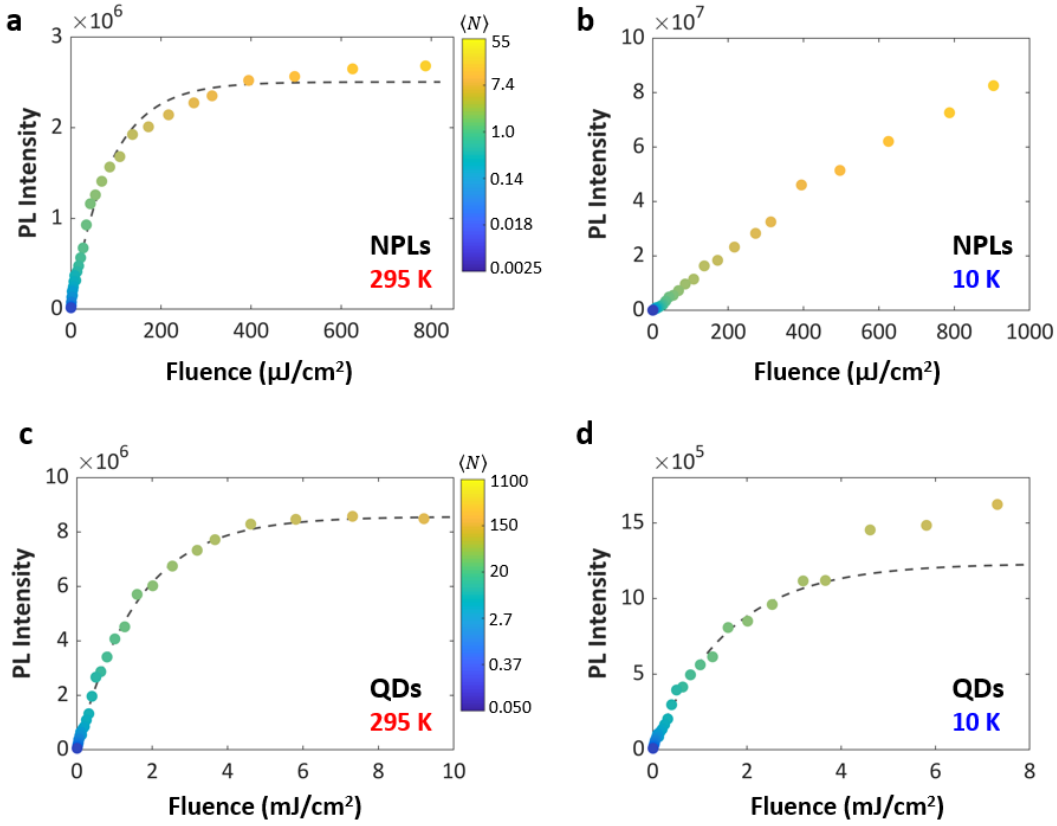

Figure 3. Static PL intensity of **(a, b)** 5.5 ML CdSe NPLs and **(c, d)** CdSe QDs at **(a, c)** 295 K and **(b, d)** 10 K as a function of 400 nm excitation fluence. Samples were dispersed in a 1:1 mixture of hexanes to methylcyclohexane at room temperature and then frozen as a glassy solid at 10 K. **(a)** As the excitation fluence of CdSe NPLs at 295 K is increased, static PL intensity saturates according to $\mathbf{1 - p_0}$ (dotted line). Color bar, which scales logarithmically with $\langle \boldsymbol{N} \rangle$, indicates the average number of excitons per NPL at each fluence based on a fitted absorption cross-section of 1.2×10^{-14} cm^2. **(b)** At 10 K, static PL intensity increases linearly as a function of fluence, indicating that nonradiative recombination is no longer dominant but rather that multiexcitons undergo radiative recombination nearly as efficiently as single excitons. **(c, d)** As the excitation fluence of CdSe QDs at 295 K is increased, PL intensity saturates.

A similar behavior is observed at 10 K. Color bar, which scales logarithmically with $\langle \boldsymbol{N} \rangle$, indicates the average number of excitons per NPL at each fluence based on a fitted absorption cross-section of 6.3×10^{-15} cm^2.

Figure 3b shows static PL intensity as a function of fluence at 10 K for the same NPL sample over the same range of fluences. Notably, at 10 K a prominent change in NPL behavior is observed relative to that at 295 K.[63,64] Instead of saturating as a function of fluence, PL intensity continues to rise approximately linearly as a function of fluence up through $\langle N \rangle \approx 20$. This linear PL intensity dependence can arise provided that low temperature emission quantum yield for single and multiexciton state approaches unity, such that NPLs containing two excitons (and even more than two excitons) undergo efficient radiative recombination at low temperatures. By comparison, the multiexciton behavior of CdSe QDs remain predominantly nonradiative upon reducing sample temperature, as shown in Figure 3d with similar saturation as at room temperature.

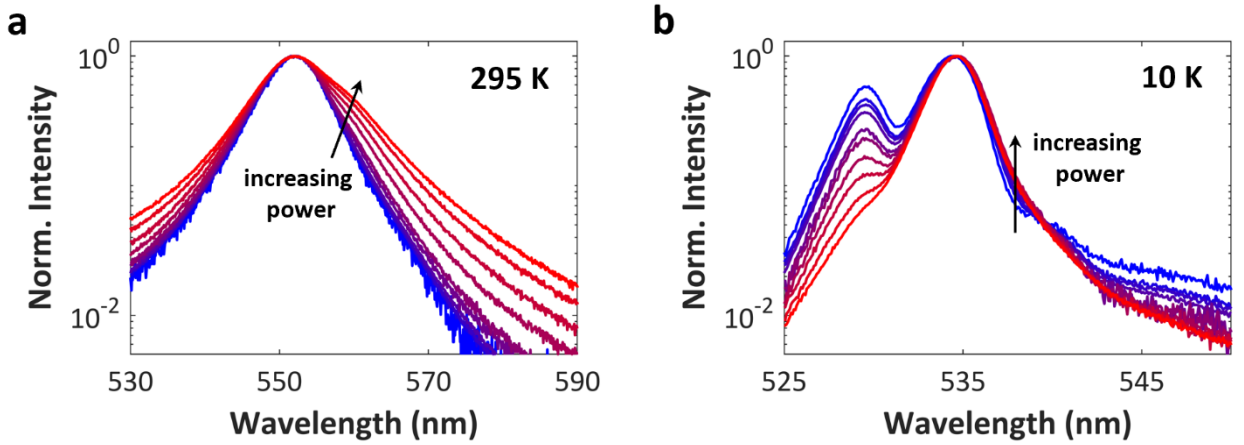

Figure 4. Static PL of 5.5 ML CdSe NPLs dispersed in a 1:1 mixture of hexanes to methylcyclohexane at **(a)** 295 K and **(b)** 10 K. Static PL traces measured as a function of pump intensity, ranging from 0.23 to 790 μJ/cm^2 ($\langle \boldsymbol{N} \rangle$ = 0.005 to 18). **(a)** At 295 K, spectral broadening is observed with a weak peak at lower energy (redder wavelength) observed, consistent with weak biexciton emission. **(b)** At 10 K, two spectral features, one corresponding to the neutral single exciton, and the other commonly attributed to a trion, are observed. Nevertheless, red-shifting owing to biexciton formation, is also present.

To further probe biexciton emission, we consider the fluence-dependent emission spectra that were evaluated in the process of generating Figure 3. Due to Coulombic binding energy, biexciton emission in core-only nanoparticles is red-shifted compared to single exciton emission. Static PL of 5.5 ML CdSe NPLs measured over a range of fluences spanning single exciton excitation through the multiexciton regime is reported in Figures 4a and 4b for both 295 K and 10 K, respectively. At 295 K, elevated fluence broadens the emission spectrum[65] from the narrower single exciton spectral profile chiefly to lower energy as a ~25

meV red-shifted biexciton that radiates weakly (see Figure S4). As broadly reported in the literature,[53–56,66–68] two emission bands are observed at low temperature, where the higher energy feature arises from single exciton radiative relaxation and the lower energy feature, here redshifted by 21.5 meV, has been argued to originate from negative trion recombination. Notably, trions are expected to radiatively recombine at twice the rate of the bright spin configuration of single excitons and do not experience spin-forbidden dark exciton states. A recent report conveys that the redder feature in 5.5 ML CdSe NPLs presents a temperature independent decay when at or below 50 K with a lifetime of 450 ps, while the single exciton decays biexponentially presenting a 30 ps bright exciton decay and 58 ns dark exciton lifetime, respectively.[55] The 30 ps bright exciton decay was ascribed to conversion of the single exciton into a triplet-like dark exciton state. Bright single excitons, then, are expected to radiate at half the trion rate and corresponding 900 ps lifetime. In our fluence-dependent PL measurements performed at 10 K, as the pump intensity is increased so that more than one electron-hole pair per NPL is excited, we find a systematic increase in amplitude of the lower energy PL feature (see Figure S3), in addition to discernible red-shifting of the lower energy feature. Provided that some fraction of NPLs remain neutral under experimental excitation conditions, these low temperature observations also convey a ~25 meV biexciton binding energy (see Figure S4) that is comparable to but larger than that of trions. Importantly, the decay of this emission is also reliably faster than the trion (as noted in Figure 2c) with a value that approaches 4 times the estimated 900 ps single bright exciton decay rate. Given the short lifetime and red-shifted emission, the data point to dominance of biexciton recombination at elevated fluence.

A remarkable feature of Figure 2c is that biexciton radiative recombination exhibits decreasing lifetime with temperature reduction in CdSe NPLs. Fast radiative decay of single excitons in CdSe NPLs has been observed previously, where temperature reduction causes a decrease in the observed single exciton lifetime.[60] This trend was justified according to a picture in which the bright singlet state is positioned a few meV higher in energy than the optically passive dark exciton state, but where enhanced oscillator strength engenders short radiative lifetimes.[56] Since biexcitons should recombine 4× faster than the bright single exciton spin configuration, such rapid single exciton recombination portends rapid biexciton recombination that can outcompete nonradiative Auger recombination. For sufficiently low temperatures whereupon recombination from the dark state imparts a 58 ns lifetime,[55] it is important to note that triplets do not prolong biexciton lifetime, since spin-allowed recombination is available to the doubly-occupied electron and hole states. The observed multiexciton decay times are also meaningfully shorter than trion decay, which is explained by the larger number of carriers involved. Indeed, with biexciton binding energies for CdSe NPLs reportedly in the range of 9-45 meV,[43,69,70] the faster radiative rate at low temperatures could suggest increased co-localization of exciton pairs within the NPL structure or influence of phonons on AR. As conveyed by Figure 2c, under the condition that thermal energy exceeds the roughly approximated

activation energy of 3.4 meV, biexcitons (as well as trions) become much less radiative and undergo AR with a rate that exceeds radiative recombination. While 3.4 meV does not correspond to available optical phonons in CdSe (near 25 meV),[71] this energy range may relate to acoustic modes associated with breathing of the thin dimension of the NPLs or rippling of the large, in-plane dimension of the particle.[72–74] Whereas the presented results show enhanced biexciton emission from these core-only NPLs, still further improved performance may be available via core/shell, gradient alloy, and related interfacial manipulations that have exhibited suppressed AR,[39,43,75] and which have been particularly successful in spherical core/shell quantum dots.[21,76,77] The especially large oscillator strengths of the bright single exciton in NPLs, which are not found in typical spherical particles, seem to permit multiexciton recombination at low temperature even in the absence of such strategies.

In conclusion, we have shown that biexciton lifetimes in CdSe NPLs decrease at cryogenic temperatures in contrast to predictions of typical Auger recombination behavior. Lifetime measurements conducted using trPL spectroscopy are complemented by PL intensity *vs* fluence dependencies. Our measurements highlight that nonradiative AR, though important at room temperature, does not dominate biexciton recombination for core-only NPLs at low temperatures. For CdSe NPLs, biexciton radiative recombination becomes significant at cryogenic temperatures and may approach unity. Furthermore, this work also highlights the unique photophysics of colloidal NPLs, which fundamentally differ from those of both bulk semiconductors and zero-dimensional nanocrystals, and continue to warrant further investigation for integration into optoelectronic devices.

Author Information

Author Contributions

N.E.W. and B.T.D. synthesized CdSe NPLs. A.B. collected, processed, and analyzed data. R.D.S. developed project idea and facilitated optical measurements. All authors contributed to the writing of this manuscript.

Notes

The authors declare no competing financial interests.

Supporting Information

Absorption and emission spectra of 5.5 ML CdSe NPLs; temperature-dependent single exciton dynamics and lifetimes; fluence-dependent Gaussian peak amplitudes of the low and high energy peaks; and biexciton binding energies extracted from fits of the biexciton emission.

Acknowledgements

This material is based upon work supported by the National Science Foundation MSN Program Award 1808590 and National Science Foundation Graduate Research Fellowship Program under Grant No. DGE-1842165 (A.B., N.E.W.). A.B. gratefully acknowledges support from a 3M Graduate Research Fellowship, the Ryan Fellowship, and the International Institute for Nanotechnology at Northwestern University. Work performed at the Center for Nanoscale Materials, a U.S. Department of Energy Office of Science User Facility, was supported by the U.S. DOE, Office of Basic Energy Sciences, under Contract No. DE-AC02-06CH11357.

References

(1) Ryu, H.-Y.; Kim, H.-S.; Shim, J.-I. Rate Equation Analysis of Efficiency Droop in InGaN Light-Emitting Diodes. *Appl. Phys. Lett.* **2009**, *95* (8), 081114.

(2) Kioupakis, E.; Rinke, P.; Delaney, K. T.; Van de Walle, C. G. Indirect Auger Recombination as a Cause of Efficiency Droop in Nitride Light-Emitting Diodes. *Appl. Phys. Lett.* **2011**, *98* (16), 161107.

(3) Cho, J.; Schubert, E. F.; Kim, J. K. Efficiency Droop in Light-Emitting Diodes: Challenges and Countermeasures. *Laser Photonics Rev.* **2013**, *7* (3), 408–421.

(4) Vaxenburg, R.; Lifshitz, E.; Efros, Al. L. Suppression of Auger-Stimulated Efficiency Droop in Nitride-Based Light Emitting Diodes. *Appl. Phys. Lett.* **2013**, *102* (3), 031120.

(5) Lim, J.; Park, Y.-S.; Wu, K.; Yun, H. J.; Klimov, V. I. Droop-Free Colloidal Quantum Dot Light-Emitting Diodes. *Nano Lett.* **2018**, *18* (10), 6645–6653.

(6) Klimov, V. I. Mechanisms for Photogeneration and Recombination of Multiexcitons in Semiconductor Nanocrystals: Implications for Lasing and Solar Energy Conversion. *J. Phys. Chem. B* **2006**, *110* (34), 16827–16845.

(7) Kambhampati, P. Multiexcitons in Semiconductor Nanocrystals: A Platform for Optoelectronics at High Carrier Concentration. *J. Phys. Chem. Lett.* **2012**, *3* (9), 1182–1190.

(8) Pietryga, J. M.; Park, Y.-S.; Lim, J.; Fidler, A. F.; Bae, W. K.; Brovelli, S.; Klimov, V. I. Spectroscopic and Device Aspects of Nanocrystal Quantum Dots. *Chem. Rev.* **2016**, *116* (18), 10513–10622.

(9) Park, Y.-S.; Bae, W. K.; Baker, T.; Lim, J.; Klimov, V. I. Effect of Auger Recombination on Lasing in Heterostructured Quantum Dots with Engineered Core/Shell Interfaces. *Nano Lett.* **2015**, *15* (11), 7319–7328.

(10) Pan, J. L. Reduction of the Auger Rate in Semiconductor Quantum Dots. *Phys. Rev. B* **1992**, *46* (7), 3977–3998.

(11) Klimov, V. I.; McBranch, D. W.; Leatherdale, C. A.; Bawendi, M. G. Electron and Hole Relaxation Pathways in Semiconductor Quantum Dots. *Phys. Rev. B* **1999**, *60* (19), 13740–13749.

(12) Robel, I.; Gresback, R.; Kortshagen, U.; Schaller, R. D.; Klimov, V. I. Universal Size-Dependent Trend in Auger Recombination in Direct-Gap and Indirect-Gap Semiconductor Nanocrystals. *Phys. Rev. Lett.* **2009**, *102* (17), 177404.

(13) Cragg, G. E.; Efros, A. L. Suppression of Auger Processes in Confined Structures. *Nano Lett.* **2010**, *10* (1), 313–317.

(14) Philbin, J. P.; Rabani, E. Electron–Hole Correlations Govern Auger Recombination in Nanostructures. *Nano Lett.* **2018**, *18* (12), 7889–7895.

(15) Kharchenko, V. A.; Rosen, M. Auger Relaxation Processes in Semiconductor Nanocrystals and Quantum Wells. *J. Lumin.* **1996**, *70* (1–6), 158–169.

(16) Haug, A. Band-to-Band Auger Recombination in Semiconductors. *J. Phys. Chem. Solids* **1988**, *49* (6), 599–605.

(17) Klimov, V. I. Quantization of Multiparticle Auger Rates in Semiconductor Quantum Dots. *Science* **2000**, *287* (5455), 1011–1013.

(18) Hollingsworth, J. A. Heterostructuring Nanocrystal Quantum Dots Toward Intentional Suppression of Blinking and Auger Recombination. *Chem. Mater.* **2013**, *25* (8), 1318–1331.

(19) Htoon, H.; Malko, A. V.; Bussian, D.; Vela, J.; Chen, Y.; Hollingsworth, J. A.; Klimov, V. I. Highly Emissive Multiexcitons in Steady-State Photoluminescence of Individual "Giant" CdSe/CdS Core/Shell Nanocrystals. *Nano Lett.* **2010**, *10* (7), 2401–2407.

(20) Dennis, A. M.; Mangum, B. D.; Piryatinski, A.; Park, Y.-S.; Hannah, D. C.; Casson, J. L.; Williams, D. J.; Schaller, R. D.; Htoon, H.; Hollingsworth, J. A. Suppressed Blinking and Auger Recombination in Near-Infrared Type-II InP/CdS Nanocrystal Quantum Dots. *Nano Lett.* **2012**, *12* (11), 5545–5551.

(21) García-Santamaría, F.; Chen, Y.; Vela, J.; Schaller, R. D.; Hollingsworth, J. A.; Klimov, V. I. Suppressed Auger Recombination in "Giant" Nanocrystals Boosts Optical Gain Performance. *Nano Lett.* **2009**, *9* (10), 3482–3488.

(22) Hou, X.; Qin, H.; Peng, X. Enhancing Dielectric Screening for Auger Suppression in CdSe/CdS Quantum Dots by Epitaxial Growth of ZnS Shell. *Nano Lett.* **2021**, *21* (9), 3871–3878.

(23) Bae, W. K.; Padilha, L. A.; Park, Y.-S.; McDaniel, H.; Robel, I.; Pietryga, J. M.; Klimov, V. I. Controlled Alloying of the Core–Shell Interface in CdSe/CdS Quantum Dots for Suppression of Auger Recombination. *ACS Nano* **2013**, *7* (4), 3411–3419.

(24) Beane, G. A.; Gong, K.; Kelley, D. F. Auger and Carrier Trapping Dynamics in Core/Shell Quantum Dots Having Sharp and Alloyed Interfaces. *ACS Nano* **2016**, *10* (3), 3755–3765.

(25) Melnychuk, C.; Guyot-Sionnest, P. Auger Suppression in N-Type HgSe Colloidal Quantum Dots. *ACS Nano* **2019**, *13* (9), 10512–10519.

(26) She, C.; Fedin, I.; Dolzhnikov, D. S.; Dahlberg, P. D.; Engel, G. S.; Schaller, R. D.; Talapin, D. V. Red, Yellow, Green, and Blue Amplified Spontaneous Emission and Lasing Using Colloidal CdSe Nanoplatelets. *ACS Nano* **2015**, *9* (10), 9475–9485.

(27) Li, Q.; Lian, T. Area- and Thickness-Dependent Biexciton Auger Recombination in Colloidal CdSe Nanoplatelets: Breaking the "Universal Volume Scaling Law." *Nano Lett.* **2017**, *17* (5), 3152–3158.

(28) Philbin, J. P.; Brumberg, A.; Diroll, B. T.; Cho, W.; Talapin, D. V.; Schaller, R. D.; Rabani, E. Area and Thickness Dependence of Auger Recombination in Nanoplatelets. *J. Chem. Phys.* **2020**, *153* (5), 054104.

(29) Guzelturk, B.; Kelestemur, Y.; Olutas, M.; Delikanli, S.; Demir, H. V. Amplified Spontaneous Emission and Lasing in Colloidal Nanoplatelets. *ACS Nano* **2014**, *8* (7), 6599–6605.

(30) Zhang, F.; Wang, S.; Wang, L.; Lin, Q.; Shen, H.; Cao, W.; Yang, C.; Wang, H.; Yu, L.; Du, Z.; Xue, J.; Li, L. S. Super Color Purity Green Quantum Dot Light-Emitting Diodes Fabricated by Using CdSe/CdS Nanoplatelets. *Nanoscale* **2016**, *8* (24), 12182–12188.

(31) Diroll, B. T.; Talapin, D. V.; Schaller, R. D. Violet-to-Blue Gain and Lasing from Colloidal CdS Nanoplatelets: Low-Threshold Stimulated Emission Despite Low Photoluminescence Quantum Yield. *ACS Photonics* **2017**, *4* (3), 576–583.

(32) Pelton, M. Carrier Dynamics, Optical Gain, and Lasing with Colloidal Quantum Wells. *J. Phys. Chem. C* **2018**, *122* (20), 10659–10674.

(33) Shin, A. J.; Hossain, A. A.; Tenney, S. M.; Tan, X.; Tan, L. A.; Foley, J. J.; Atallah, T. L.; Caram, J. R. Dielectric Screening Modulates Semiconductor Nanoplatelet Excitons. *J. Phys. Chem. Lett.* **2021**, *12* (20), 4958–4964.

(34) Li, Q.; Yang, Y.; Que, W.; Lian, T. Size- and Morphology-Dependent Auger Recombination in $CsPbBr_3$ Perovskite Two-Dimensional Nanoplatelets and One-Dimensional Nanorods. *Nano Lett.* **2019**, *19* (8), 5620–5627.

(35) Gramlich, M.; Bohn, B. J.; Tong, Y.; Polavarapu, L.; Feldmann, J.; Urban, A. S. Thickness-Dependence of Exciton–Exciton Annihilation in Halide Perovskite Nanoplatelets. *J. Phys. Chem. Lett.* **2020**, *11* (13), 5361–5366.

(36) Kunneman, L. T.; Tessier, M. D.; Heuclin, H.; Dubertret, B.; Aulin, Y. V.; Grozema, F. C.; Schins, J. M.; Siebbeles, L. D. A. Bimolecular Auger Recombination of Electron–Hole Pairs in Two-Dimensional CdSe and CdSe/CdZnS Core/Shell Nanoplatelets. *J. Phys. Chem. Lett.* **2013**, *4* (21), 3574–3578.

(37) Grim, J. Q.; Christodoulou, S.; Di Stasio, F.; Krahne, R.; Cingolani, R.; Manna, L.; Moreels, I. Continuous-Wave Biexciton Lasing at Room Temperature Using Solution-Processed Quantum Wells. *Nat. Nanotechnol.* **2014**, *9* (11), 891–895.

(38) Baghani, E.; O'Leary, S. K.; Fedin, I.; Talapin, D. V.; Pelton, M. Auger-Limited Carrier Recombination and Relaxation in CdSe Colloidal Quantum Wells. *J. Phys. Chem. Lett.* **2015**, *6* (6), 1032–1036.

(39) Ma, X.; Diroll, B. T.; Cho, W.; Fedin, I.; Schaller, R. D.; Talapin, D. V.; Gray, S. K.; Wiederrecht, G. P.; Gosztola, D. J. Size-Dependent Biexciton Quantum Yields and Carrier Dynamics of Quasi-Two-Dimensional Core/Shell Nanoplatelets. *ACS Nano* **2017**, *11* (9), 9119–9127.

(40) Pelton, M.; Andrews, J. J.; Fedin, I.; Talapin, D. V.; Leng, H.; O'Leary, S. K. Nonmonotonic Dependence of Auger Recombination Rate on Shell Thickness for CdSe/CdS Core/Shell Nanoplatelets. *Nano Lett.* **2017**, *17* (11), 6900–6906.

(41) Vale, B. R. C.; Socie, E.; Burgos-Caminal, A.; Bettini, J.; Schiavon, M. A.; Moser, J.-E. Exciton, Biexciton, and Hot Exciton Dynamics in $CsPbBr_3$ Colloidal Nanoplatelets. *J. Phys. Chem. Lett.* **2020**, *11* (2), 387–394.

(42) Villamil Franco, C.; Mahler, B.; Cornaggia, C.; Gustavsson, T.; Cassette, E. Auger Recombination and Multiple Exciton Generation in Colloidal Two-Dimensional Perovskite Nanoplatelets: Implications for Light-Emitting Devices. *ACS Appl. Nano Mater.* **2021**, *4* (1), 558–567.

(43) Peng, L.; Cho, W.; Zhang, X.; Talapin, D.; Ma, X. Observation of Biexciton Emission from Single Semiconductor Nanoplatelets. *Phys. Rev. Mater.* **2021**, *5* (5), L051601.

(44) Chepic, D. I.; Efros, Al. L.; Ekimov, A. I.; Ivanov, M. G.; Kharchenko, V. A.; Kudriavtsev, I. A.; Yazeva, T. V. Auger Ionization of Semiconductor Quantum Dots in a Glass Matrix. *J. Lumin.* **1990**, *47*, 113–127.

(45) Kobayashi, Y.; Tamai, N. Size-Dependent Multiexciton Spectroscopy and Moderate Temperature Dependence of Biexciton Auger Recombination in Colloidal CdTe Quantum Dots. *J. Phys. Chem. C* **2010**, *114* (41), 17550–17556.

(46) Hyeon-Deuk, K.; Kobayashi, Y.; Tamai, N. Evidence of Phonon-Assisted Auger Recombination and Multiple Exciton Generation in Semiconductor Quantum Dots Revealed by Temperature-Dependent Phonon Dynamics. *J. Phys. Chem. Lett.* **2014**, *5* (1), 99–105.

(47) Hausser, S.; Fuchs, G.; Hangleiter, A.; Streubel, K.; Tsang, W. T. Auger Recombination in Bulk and Quantum Well InGaAs. *Appl. Phys. Lett.* **1990**, *56* (10), 913–915.

(48) Lui, W. W.; Yamanaka, T.; Yoshikuni, Y.; Seki, S.; Yokoyama, K. Unifying Explanation for Recent Temperature Sensitivity Measurements of Auger Recombination Effects in Strained InGaAs/InGaAsP Quantum-well Lasers. *Appl. Phys. Lett.* **1993**, *63* (12), 1616–1618.

(49) Fuchs, G.; Schiedel, C.; Hangleiter, A. Auger Recombination in Strained and Unstrained InGaAs/InGaAsP Multiple Quantum-well Lasers. *Appl. Phys. Lett.* **1993**, *62*, 396.

(50) Zou, Y.; Osinski, J. S.; Grodzinski, P.; Dapkus, P. D.; Rideout, W.; Sharfin, W. F.; Crawford, F. D. Effect of Auger Recombination and Differential Gain on the Temperature Sensitivity of 1.5 Mm Quantum Well Lasers. *Appl. Phys. Lett.* **1993**, *62* (2), 175–177.

(51) Seki, S.; Lui, W. W.; Yokoyama, K. Explanation for the Temperature Insensitivity of the Auger Recombination Rates in 1.55 Mm InP-based Strained-layer Quantum-well Lasers. *Appl. Phys. Lett.* **1995**, *66* (23), 3093–3095.

(52) Zegrya, G. G.; Polkovnikov, A. S. Mechanisms of Auger Recombination in Quantum Wells. *J. Exp. Theor. Phys.* **1998**, *86* (4), 815–832.

(53) Achtstein, A. W.; Scott, R.; Kickhöfel, S.; Jagsch, S. T.; Christodoulou, S.; Bertrand, G. H. V.; Prudnikau, A. V.; Antanovich, A.; Artemyev, M.; Moreels, I.; Schliwa, A.; Woggon, U. P -State Luminescence in CdSe Nanoplatelets: Role of Lateral Confinement and a Longitudinal Optical Phonon Bottleneck. *Phys. Rev. Lett.* **2016**, *116* (11), 116802.

(54) Diroll, B. T.; Cho, W.; Coropceanu, I.; Harvey, S. M.; Brumberg, A.; Holtgrewe, N.; Crooker, S. A.; Wasielewski, M. R.; Prakapenka, V. B.; Talapin, D. V.; Schaller, R. D. Semiconductor Nanoplatelet Excimers. *Nano Lett.* **2018**, *18* (11), 6948–6953.

(55) Shornikova, E. V.; Yakovlev, D. R.; Biadala, L.; Crooker, S. A.; Belykh, V. V.; Kochiev, M. V.; Kuntzmann, A.; Nasilowski, M.; Dubertret, B.; Bayer, M. Negatively Charged Excitons in CdSe Nanoplatelets. *Nano Lett.* **2020**, *20* (2), 1370–1377.

(56) Antolinez, F. V.; Rabouw, F. T.; Rossinelli, A. A.; Keitel, R. C.; Cocina, A.; Becker, M. A.; Norris, D. J. Trion Emission Dominates the Low-Temperature Photoluminescence of CdSe Nanoplatelets. *Nano Lett.* **2020**, *20* (8), 5814–5820.

(57) Peng, L.; Otten, M.; Hazarika, A.; Coropceanu, I.; Cygorek, M.; Wiederrecht, G. P.; Hawrylak, P.; Talapin, D. V.; Ma, X. Bright Trion Emission from Semiconductor Nanoplatelets. *Phys. Rev. Mater.* **2020**, *4* (5), 056006.

(58) Ayari, S.; Quick, M. T.; Owschimikow, N.; Christodoulou, S.; Bertrand, G. H. V.; Artemyev, M.; Moreels, I.; Woggon, U.; Jaziri, S.; Achtstein, A. W. Tuning Trion Binding Energy and Oscillator Strength in a Laterally Finite 2D System: CdSe Nanoplatelets as a Model System for Trion Properties. *Nanoscale* **2020**, *12* (27), 14448–14458.

(59) Benjamin, E.; Yallapragada, V. J.; Amgar, D.; Yang, G.; Tenne, R.; Oron, D. Temperature Dependence of Excitonic and Biexcitonic Decay Rates in Colloidal Nanoplatelets by Time-Gated Photon Correlation. *J. Phys. Chem. Lett.* **2020**, *11* (16), 6513–6518.

(60) Ithurria, S.; Tessier, M. D.; Mahler, B.; Lobo, R. P. S. M.; Dubertret, B.; Efros, Al. L. Colloidal Nanoplatelets with Two-Dimensional Electronic Structure. *Nat. Mater.* **2011**, *10* (12), 936–941.

(61) Yang, Y. A.; Wu, H.; Williams, K. R.; Cao, Y. C. Synthesis of CdSe and CdTe Nanocrystals without Precursor Injection. *Angew. Chem. Int. Ed.* **2005**, *44* (41), 6712–6715.

(62) Tessier, M. D.; Javaux, C.; Maksimovic, I.; Loriette, V.; Dubertret, B. Spectroscopy of Single CdSe Nanoplatelets. *ACS Nano* **2012**, *6* (8), 6751–6758.

(63) Van Dao, L.; Wen, X.; Do, M. T. T.; Hannaford, P.; Cho, E.-C.; Cho, Y. H.; Huang, Y. Time-Resolved and Time-Integrated Photoluminescence Analysis of State Filling and Quantum Confinement of Silicon Quantum Dots. *J. Appl. Phys.* **2005**, *97* (1), 013501.

(64) Makarov, N. S.; Guo, S.; Isaienko, O.; Liu, W.; Robel, I.; Klimov, V. I. Spectral and Dynamical Properties of Single Excitons, Biexcitons, and Trions in Cesium–Lead-Halide Perovskite Quantum Dots. *Nano Lett.* **2016**, *16* (4), 2349–2362.

(65) Pelton, M.; Ithurria, S.; Schaller, R. D.; Dolzhnikov, D. S.; Talapin, D. V. Carrier Cooling in Colloidal Quantum Wells. *Nano Lett.* **2012**, *12* (12), 6158–6163.

(66) Tessier, M. D.; Biadala, L.; Bouet, C.; Ithurria, S.; Abecassis, B.; Dubertret, B. Phonon Line Emission Revealed by Self-Assembly of Colloidal Nanoplatelets. *ACS Nano* **2013**, *7* (4), 3332–3340.

(67) Biadala, L.; Liu, F.; Tessier, M. D.; Yakovlev, D. R.; Dubertret, B.; Bayer, M. Recombination Dynamics of Band Edge Excitons in Quasi-Two-Dimensional CdSe Nanoplatelets. *Nano Lett.* **2014**, *14* (3), 1134–1139.

(68) Shornikova, E. V.; Biadala, L.; Yakovlev, D. R.; Sapega, V. F.; Kusrayev, Y. G.; Mitioglu, A. A.; Ballottin, M. V.; Christianen, P. C. M.; Belykh, V. V.; Kochiev, M. V.; Sibeldin, N. N.; Golovatenko, A. A.; Rodina, A. V.; Gippius, N. A.; Kuntzmann, A.; Jiang, Y.; Nasilowski, M.; Dubertret, B.; Bayer, M. Addressing the Exciton Fine Structure in Colloidal Nanocrystals: The Case of CdSe Nanoplatelets. *Nanoscale* **2018**, *10* (2), 646–656.

(69) Morgan, D. P.; Maddux, C. J. A.; Kelley, D. F. Transient Absorption Spectroscopy of CdSe Nanoplatelets. *J. Phys. Chem. C* **2018**, *122* (41), 23772–23779.

(70) Geiregat, P.; Tomar, R.; Chen, K.; Singh, S.; Hodgkiss, J. M.; Hens, Z. Thermodynamic Equilibrium between Excitons and Excitonic Molecules Dictates Optical Gain in Colloidal CdSe Quantum Wells. *J. Phys. Chem. Lett.* **2019**, *10* (13), 3637–3644.

(71) Cherevkov, S. A.; Fedorov, A. V.; Artemyev, M. V.; Prudnikau, A. V.; Baranov, A. V. Anisotropy of Electron-Phonon Interaction in Nanoscale CdSe Platelets as Seen via off-Resonant and Resonant Raman Spectroscopy. *Phys. Rev. B* **2013**, *88* (4), 041303.

(72) Girard, A.; Saviot, L.; Pedetti, S.; Tessier, M. D.; Margueritat, J.; Gehan, H.; Mahler, B.; Dubertret, B.; Mermet, A. The Mass Load Effect on the Resonant Acoustic Frequencies of Colloidal Semiconductor Nanoplatelets. *Nanoscale* **2016**, *8* (27), 13251–13256.

(73) Girard, A.; Margueritat, J.; Saviot, L.; Machon, D.; Mahler, B.; Tessier, M. D.; Pedetti, S.; Dubertret, B.; Géhan, H.; Jeanneau, E.; Vera, R.; Mermet, A. Environmental Effects on the Natural Vibrations of Nanoplatelets: A High Pressure Study. *Nanoscale* **2017**, *9* (19), 6551–6557.

(74) Mork, A. J.; Lee, E. M. Y.; Tisdale, W. A. Temperature Dependence of Acoustic Vibrations of CdSe and CdSe–CdS Core–Shell Nanocrystals Measured by Low-Frequency Raman Spectroscopy. *Phys. Chem. Chem. Phys.* **2016**, *18* (41), 28797–28801.

(75) Jiang, Y.; Cui, M.; Li, S.; Sun, C.; Huang, Y.; Wei, J.; Zhang, L.; Lv, M.; Qin, C.; Liu, Y.; Yuan, M. Reducing the Impact of Auger Recombination in Quasi-2D Perovskite Light-Emitting Diodes. *Nat. Commun.* **2021**, *12* (1), 336.

(76) Nasilowski, M.; Spinicelli, P.; Patriarche, G.; Dubertret, B. Gradient CdSe/CdS Quantum Dots with Room Temperature Biexciton Unity Quantum Yield. *Nano Lett.* **2015**, *15* (6), 3953–3958.

(77) Javaux, C.; Mahler, B.; Dubertret, B.; Shabaev, A.; Rodina, A. V.; Efros, Al. L.; Yakovlev, D. R.; Liu, F.; Bayer, M.; Camps, G.; Biadala, L.; Buil, S.; Quelin, X.; Hermier, J.-P. Thermal Activation of Non-Radiative Auger Recombination in Charged Colloidal Nanocrystals. *Nat. Nanotechnol.* **2013**, *8* (3), 206–212.

Table of Contents Graphic